South African Journal of Chemical Engineering 40 (2022) 144–153

Contents lists available at ScienceDirect

South African Journal of Chemical Engineering

journal homepage: www.elsevier.com/locate/sajce

Surface functionalized plant residue in cu2+ scavenging: Chemometrics of operational parameters for process economy validation

Adejumoke A. INYINBOR [a,*], Folahan A. Adekola [b], Olugbenga S. Bello [a,c], Deborah T. Bankole [a], Toyin A. Oreofe [d], Adewale F. Lukman [a], Gabriel A. Olatunji [b]

[a] Department of Physical Sciences, Landmark University, P.M.B 1001, Omu Aran, Nigeria.
[b] Department of Industrial Chemistry, University of Ilorin, P.M.B 1515, Ilorin, Nigeria.
[c] Department of Pure and Applied Chemistry, Faculty of Sciences, Ladoke Akintola University of Technology, P.M.B. 4000, Ogbomoso, Nigeria.
[d] Department of Chemical Engineering, College of Engineering, Landmark University, P.M.B 1001, Omu Aran, Nigeria.

ARTICLE INFO

Keywords:
Irvingia gabonensis, Chemometrics
Cu^{2+}
Process economy

ABSTRACT

Wastes obtained from the nuts of dika fruits (Irvingia gabonensis) were treated with EDTA in surface functionalization for the adsorption of Cu2+. EDTA functionalized Irvingia gabonensis (EIG) showed strong stretching vibration of C=O. Morphological appearance of EIG showed fibrous appearance of agrowastes while the Branneur-Emmer-Teller (BET) surface area was low. Optimum pH was obtained to be 5 while adsorption equilibrium time was rapid. The adsorption data fitted best into the Freundlich adsorption isotherm and the Langmuir maximum monolayer adsorption capacity was 73.53 mg/g. The Pseudo-second order kinetics model best described the kinetics of the Cu2+-EIG adsorption system. The adsorption energy of the Dubinin-Radushkevich modeling was 5.51 kJ/mol, indicating that Cu2+ uptake onto EIG was a more of physical in nature. Correlation analysis validated the strength of relationship between concentration, equilibrium time and quantity adsorbed. The regression model estimated using the ordinary least square estimator (OLSE) indicates that every 1 unit temperature change will cause a 20.5 % uptake of Cu2+ thus presented an economical process.

1. Introduction

Water pollution continues as a global challenge posing serious threat on flora and ecology as well as affecting the health of human and other living organisms (Kajeiou et al., 2020). High levels of toxic pollutants are released into the water bodies from agricultural and industrial runoff, these pollutants may include heavy metals (Flanagan et al., 2019; Kajeiou et al., 2020). High concentration of heavy metal may present extreme danger to living organisms (Siddiqui, 2018) and creates environmental harms (Soliman et al., 2019). For instance, the high solubility of copper enhances its continuous deposition in food chain, human brain, pancreas, myocardium and liver (El-Shafey et al., 2017).

Copper has found wide use in various industries including fungicide preparation, algae control in raw water, dye mordants and additives in book binding pastes. Copper is however considered as one of the most toxic chemicals (Fawzy, 2020). Hence, effluents from copper utilizing industries must be thoroughly rid-off this danger before eventual discharge into the aquatic systems (Fawzy, 2020; Inyinbor, et al., 2019).

A couple of techniques such as ion exchange (Tavakoli et al., 2017), membrane separation, chemical precipitation (Gajda et al., 2017), reverse osmosis, oxidation and adsorption process (Lucaci et al., 2019), have been employed for the removal of copper from the water environment (Fawzy, 2020). However, diverse limitations such as partial metal removal, high energy cost, and formation of toxic byproducts exists with the aforementioned techniques (Fazlzadeh et al., 2017). Adsorption using activated carbon has continued to be a preferred choice because of its efficiency and easy operational management (Inyinbor et al., 2019; Lin et al., 2019; Xiong et al., 2019). Expensive activated carbon however has limited access and usage of adsorption technique (Inyinbor et al., 2019). Generating alternative to activated carbon from a renewable and cheap source is no doubt an answer to the current global water pollution challenge thus can never be overemphasized.

Agricultural wastes with surface functional groups and distinct fibrous nature present characteristics that is suitable for pollutants uptake. Surface modification and functionalization may also enhance agrowaste pollutant uptake efficiency.

Here, the surface of bioadsorbent prepared from the wastes of

* Corresponding author.
E-mail address: nyinbor.adejumoke@landmarkuniversity.edu.ng (A.A. INYINBOR).

https://doi.org/10.1016/j.sajce.2022.03.001
Received 6 June 2021; Received in revised form 15 February 2022; Accepted 2 March 2022
Available online 4 March 2022

Irvingia gabonensis seed was modified with EDTA. We aimed at taking advantage of the possible claw surface that EDTA is able to provide; as well as its adsorption and precipitation properties for the removal of copper ions from aqueous solution. In order to establish the applicability of the prepared adsorbent, operational parameters as well as isothermal, kinetics, thermodynamics and reusability studies were also carried. The interrelation of time and temperature with quantity of Cu^{2+} adsorbed were statistically established to ascertain process economy.

2. Materials and methods

2.1. Plant residue collection, pretreatment and surface functionalization

Irvingia gabonensis endocarp was purchased from local farmers in Omu Aran, Kwara State, Nigeria, located on latitude 8.1402° N and longitude 5.0963° E. *Irvingia gabonensis* endocarp waste (IG) were neatly separated from its soup recipe content. IG were effectively washed and water/moisture were removed by overnight drying in a mild temperature oven. Dried IG were smoothly pulverized and reduced to a particle size 150-250μm through appropriate sieve. A 29.255g of EDTA was dissolved to make a liter of 0.1 M EDTA solution. The acid which was completely brought into solution using few pellets of NaOH was contacted with IG in a ratio of 10:1. The contact done at room temperature was left to agitate for 24 hours. The mixture was filtered, thoroughly washed to remove ungrafted acid and subsequently dried in a low temperature controlled oven. The dried sample was stored in a tight container and labeled EIG.

2.2. Adsorbent characteristics

Surface morphology and topography of EIG pre and post Cu^{2+} adsorption were obtained using a FEIESEM quanta 200 for SEM whose focus was set to about 10 mm and the accelerating voltage ranged between 12.5 and 15.0 kV, image of 2000 magnification was selected for discussion. Adsorbent pore diameter as well as BET surface area were determined using a Micrometric Tristar II for surface area and porosity analysis.

2.3. Cu^{2+} stock solution

Accurate mass (3.931 g) of an analar grade of $CuSO_4.5H_2O$ (Lobal Chemie, India) was made into a liter stock solution (1000 mg/L Cu^{2+}). Other lower concentrations solutions required for adsorption were prepared from the stock solution.

2.4. Batch adsorption studies

Varying the adsorption operational parameters gives clue into adsorbent applicability. Batch adsorption systems were operated with varying pH (2 to 5.5), adsorbent dosage (1 to 5g/L), temperature (40-80 °C), contact time (1 to 120 min), and system speed (150 to 300 rpm). Salinity of the adsorption system was investigated by the addition of NaCl of concentrations 0.001 M, 0.01 M and 0.1 M. Accurately weighed mass of EIG was added to a 100 cm^3 of a known concentration of Cu^{2+} solution, this mixture was sealed in plastic bottles. The mixture was agitated at specific speed and a fixed temperature, using a thermostated water bath shaker, until equilibrium is achieved. The spent adsorbent was separated by filtration and atomic absorption spectrophotometer (AAS) was employed in analyzing the residual metal ion concentration. The quantity adsorbed was evaluated using Eq. (1).

$$q_t = \frac{(C_i - C_t)}{M} \; X \; V \tag{1}$$

While the percentage adsorbed was calculated using the mathematical expression Eq.(2).

$$\%\ Removal = \frac{(C_i - C_t)}{C_t} \; X \; 100 \tag{2}$$

Where C_i and C_t = initial concentration of the metal ion and the concentration at time, t respectively. M = mass of EIG in (grams) and V = the volume of Cu^{2+} in liters.

2.5. Spent adsorption regeneration

The reusability/regeneration study of the spent adsorbent was conducted using water, HCl (0.1 M) and CH_3COOH (0.1 M) as the desorbing agents. A 0.1 g of the preloaded EIG was added to 100 cm^3 of each desorbing agent, in separate plastic bottles. These mixtures were agitated for 120 minutes in a thermostated shaker whose temperature and speed were fixed at 26 °C and 150 rpm respectively. The concentration of Cu^{2+} desorbed was analyzed with AAS. The mathematical equation (3) was used for calculating percentage desorption efficiency.

$$Desorption\ efficiency\ (\%) = \frac{q_{de}}{q_{ad}} \; X \; 100 \tag{3}$$

Where q_{ad} and q_{de} are quantity adsorbed and quantity desorbed respectively.

2.6. Mathematical modeling of Adsorption

2.6.1. Isothermal models

Understanding the mechanism of Cu^{2+} uptake could give insight into the possible column packing technique. Isothermal studies provides insight into mechanism and modes of EIG-Cu^{2+} interactions. Equilibrium data were therefore analyzed with Langmuir Langmuir, 1917), Freundlich (Freundlich, 1906), Temkin (Vinet and Zhedanov, 2011) and Dubinin-Radushkevich (Dubinin and Radushkevich, 1947) whose equations as represented as (4; 4a), ((5), (6) and (7; 7a & 7b) respectively.

$$\frac{C_e}{q_e} = \frac{1}{q_{max}K_L} + \frac{C_e}{q_{max}} \tag{4}$$

$$R_L = \frac{1}{(1 + K_L C_o)} \tag{4a}$$

$$Logq_e = \frac{1}{n} logC_e + \log K_F \tag{5}$$

$$q_e = BlnA_T + BlnC_e \tag{6}$$

$$lnq_e = lnq_o - \beta\varepsilon^2 \tag{7}$$

$$\varepsilon = RTln\left(1 + \frac{1}{ce}\right) \tag{7a}$$

$$E = \frac{1}{\sqrt{2\beta}} \tag{7b}$$

q_e = the amount of Cu^{2+} adsorbed onto the surface of the adsorbent at equilibrium (mg/g), q_{max} = the maximum adsorption capacity (Langmuir) (mg/g), C_e = the concentration at equilibrium (mg/L), k_f and n are Freundlich constants, k_L is the Langmuir adsorption constant, A = Temkin constant (L/g), $B = R_T/b$, a and b are related to the heat of adsorption, β = the activity coefficient, R = the gas constant (8.314 J/mol K) and T = the temperature (K).

2.6.2. Kinetic models

The kinetic data were analyzed using the Elovich model Aharoni and Ungarish, 1976), pseudo first order (Lagergren, 1898), pseudo second order (Ho and McKay, 1999), Avrami model (Avrami, 1940), fractional power and Intraparticle diffusion model (Weber, 1963) as presented in Eqs (8), ((9), (10), (11), (12) and (13).

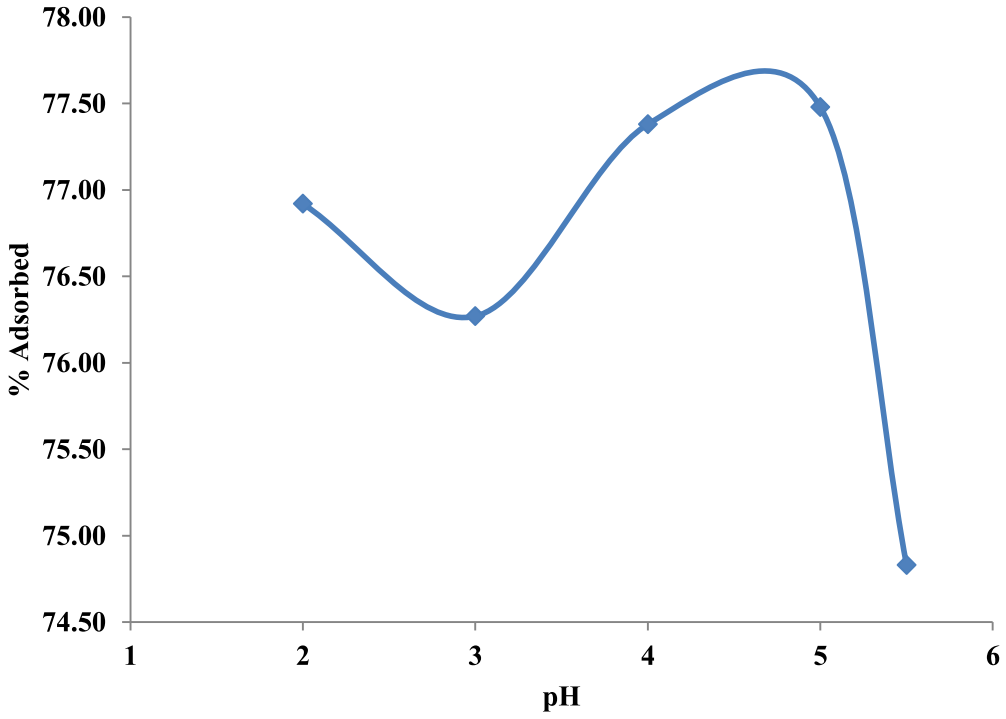

Fig. 1. Effects of varying pH on EIG efficiency for Cu2+ uptake.Conditions: Temperature (26°C), Adsorbent dose (1g/L), agitation time (120 minutes), agitation speed (200 rpm) and a 60 mg/L Cu2+ concentration.

$$q_t = \frac{1}{\beta}\ln(\alpha\beta) + \frac{1}{\beta}lnt \quad (8)$$

$$\ln(q_e - q_t) = lnq_e - k_1 t \quad (9)$$

$$\frac{t}{q_e} = \frac{1}{K_2 q_e} + \frac{1}{q_e t} \quad (10)$$

$$ln[-\ln(1-\alpha)] = lnk_{Av} + n_{Av} lnt \quad (11)$$

$$q_t = K_{id} t^{1/2} + C \quad (12)$$

$$logq_t = logK_{id} + vlogt \quad (13)$$

2.6.3. Statistical data validation

2.6.3.1. Kinetics data validation. Statistical methods such as Chi square (X^2) and Sum Square of Error (SSE) were tools used to validate the kinetic data, represented as Eqs. (14) and (15).

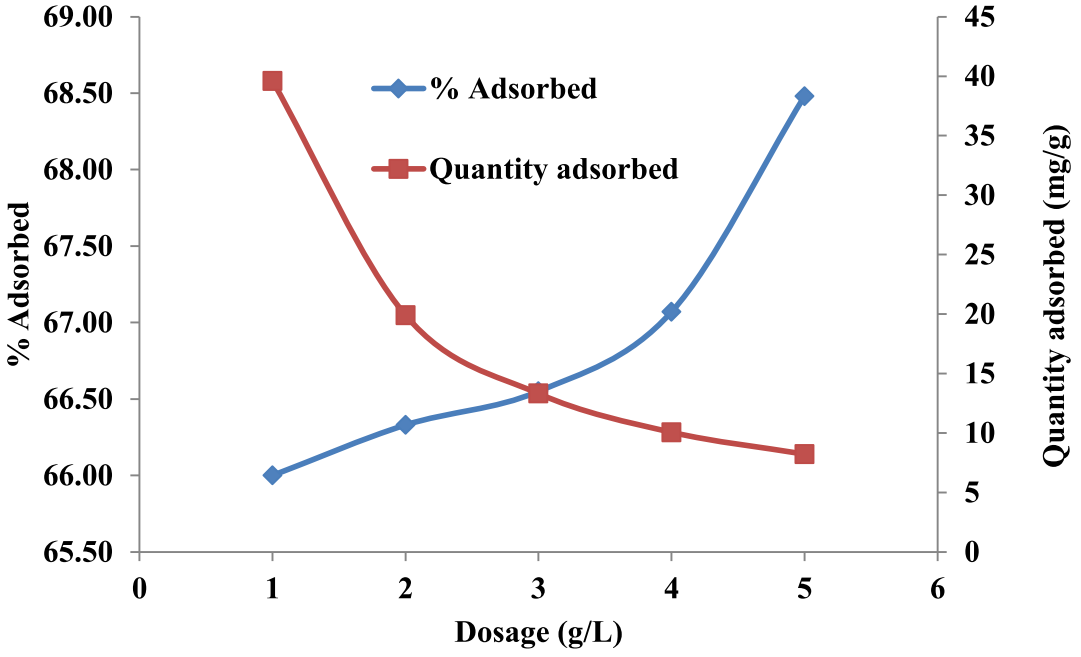

Fig. 2. Effects of varying dosage of EIG in the efficiency of Cu^{2+} uptake. Conditions: Temperature (26°C), a 60 mg/L Cu^{2+} solution, pH 5, agitation time (120 minutes), agitation speed (200 rpm).

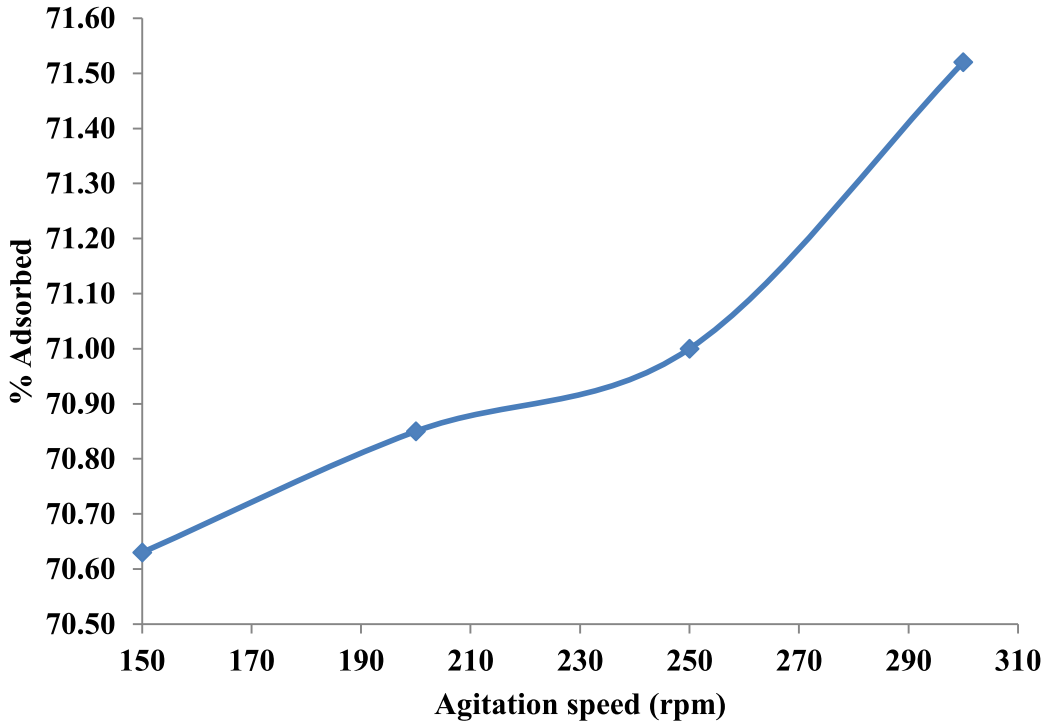

Fig. 3. Agitation speed variation of Cu^{2+}-EIG system on the EIG efficiency for Cu^{2+}uptake. Conditions: pH 5, Dosage (1 g/L), Temperature (26°C), agitation time (120 minutes) and a 60 mg/L Cu^{2+} solution.

$$SSE = \sum_{i=1}^{n} \left(q_{cal} - q_{exp}\right)^2 \quad (14)$$

$$X^2 = \sum_{i=1}^{n} \frac{\left(q_{exp} - q_{cal}\right)^2}{q_{cal}} \quad (15)$$

2.6.3.2. Statistical analysis of process operational parameters. The correlation analysis was employed to assess the strength of the relationship between two variables using the correlation coefficient. The correlation coefficient between variable *X* and *Y* is denoted by ρ and mathematically defined by mathematical relation (1) of supplementary data.

We adopted the regression model to explore the relationship between the dependent variable Y and one or more independent variables. The

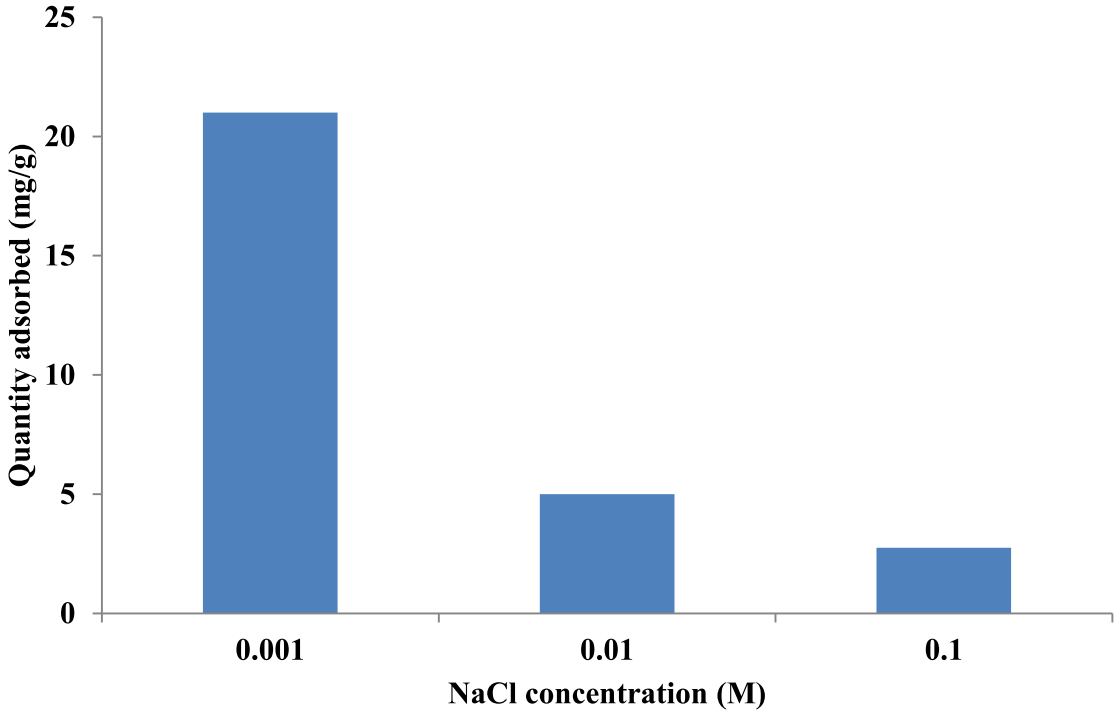

Fig. 4. Salinity effects of Cu2+-EIG system on the EIG efficiency for Cu2+uptake.. Conditions: Temperature 27 °C, Dosage (1 g/L), a 60 mg/L Cu2+ solution, Agitation speed (200 rpm), agitation time (120 minutes), pH 5.

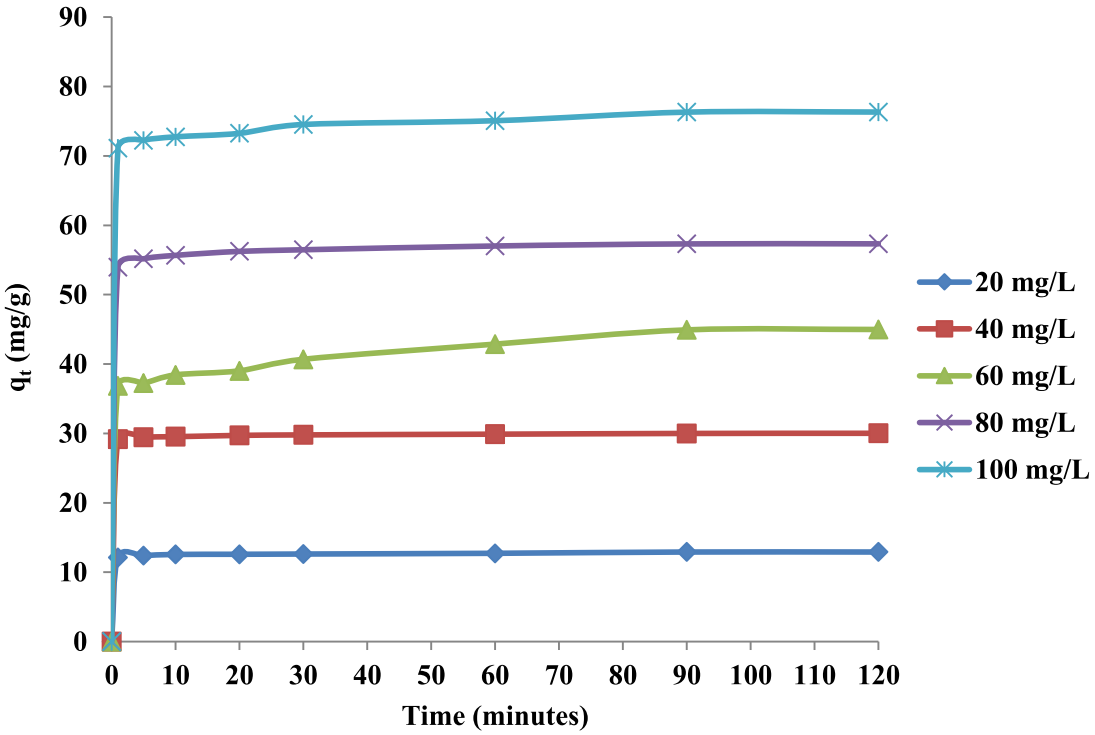

Fig. 5. Contact time and Cu2+ solution concentrations effects on the efficiency of EIG for Cu2+uptake. Conditions: pH 5, Agitation speed (200 rpm), Adsorbent dose (1g/L), agitation time (120 minutes), Temperature (26 °C),.

parameters in the model were estimated using the ordinary least squares estimator. The adequacy of the model was ascertained using the F-test. The statistical analysis was conducted using R and SPSS Statistics 22.

2.6.4. Thermodynamics studies

The enthalpy of adsorption ΔH^o, Gibb's free energy ΔG^o and entropy ΔS^o were evaluated using Eqs. (16) and (17).

$$\Delta G^o = -RTlnK_o \tag{16}$$

$$lnK_o = \frac{\Delta S^o}{R} - \frac{\Delta H^o}{RT} \tag{17}$$

3. Results and discussion

3.1. Effects of operation parameters on adsorption of Cu^{2+} on EIG

3.1.1. pH effects on Cu^{2+} uptake onto EIG

Adsorbate pH media greatly influences the behavior of the adsorbent as well as the form in which adsorbate exists in solution. For instance, copper exists in solution at low pH (pH < 6) while precipitation of Cu $(OH)_2$ may result at pH greater than 5. The percentage Cu^{2+} removal increased as the initial pH increased from pH 2, optimum percentage Cu^{2+} removal (77.48 %) was obtained at pH 5(Fig. 1). Due to the drastic decrease in Cu^{2+} uptake onto EIG cum possible $Cu(OH)_2$ precipitation at pH greater than 5, studies on pH effect studies was limited to pH range between 1 and 5.5. The pHpzc of EIG as detailed in our previous report was obtained to be 2 (Inyinbor et al., 2015). EIG surface is expected to be positively charged below the pHpzc and negatively charged above the pHpzc. The attraction force between the positively charged Cu^{2+} and negatively charged EIG surface, results into Cu^{2+} adsorption as the pH increased. Other researchers utilizing agrowaste such as date palm (El-Shafey et al., 2017) and *Lessonia nigrecens* (Cid et al., 2018) as adsorbent previously reported optimum adsorption at pH 5.

3.1.2. of varying dose of EIG on Cu^{2+} removal

Increased quantity of EIG present more surface area hence Cu^{2+} percentage removal increased from 66 % to 68.48 % as the adsorbent dosage increases from 1 to 5 g/L as (Fig. 2). The uptake of Cu^{2+} onto a unit mass of EIG decreased from 39.60 mg/g to 8.22 mg/g as EIG dose increased from 1 to 5 g/L. The variation in concentration gradient of adsorbate and adsorbent may have resulted into decrease in quantity adsorbed as adsorbent dosage increased, Hayati et al. (Hayati et al., 2017).

3.1.3. Effects of varying speed of Cu^{2+} bombardment on EIG surface

Agitation speed slightly increased percentage removal of Cu^{2+} from 70.63 to 71.52 % (Fig. 3). The increase in the agitation speed of the Cu^{2+}-EIG system increased Cu^{2+} collision with EIG surface thus more Cu^{2+} gained access to various EIG adsorption sites. Hence, an increase in percentage adsorption, at elevated agitation speed.

3.1.4. Salinity effects on Cu^{2+} uptake onto EIG

Increase in the solution salinity resulted into quantity of Cu^{2+} adsorbed onto EIG. Hence, percentage adsorbed decreased from 33.78 mg/g to 2.75 mg/g as NaCl concentration increased from 0.001 M to 0.1 M (Fig. 4). The contest for available adsorption site on EIG by two cationic specie (Cu^{2+} and Na^+) may be the reason for the reduction in quantity of Cu^{2+} adsorbed at high concentration of NaCl. Effects of competing is usually non-significant when pollutant removal technique follows precipitation or covalent bonding. However, competing ion effect is greatly pronounced for ion exchange or complex formation adsorption processes. Decrease in quantity adsorbed as the concentration of competing ion increased has previously been reported by Tan et al. (Tan et al., 2015)

3.1.5. Contact time and initial concentration effects on Cu^{2+} uptake onto EIG

Initial concentration effects was varied with concentration, quantities of Cu^{2+} removal increased in a direct proportion with the Cu^{2+} initial concentration. Rapid equilibrium was observed and quantities

Table 1
Comparing the adsorption potential of EIG to previous literature reports.

Adsorbents	q_{max} (mg/g)	References
Farmyard manure char	44.50	(Batool et al., 2017)
Poultry manure char	43.68	(Batool et al., 2017)
Modified bentonite	27.00	(De Castro et al., 2018)
Goose berry seeds activated carbon	66.79	(Mondal and Majumder, 2019)
Treated fish waste	2.10	(El Haouti et al., 2019)
Acid treated dika nut	103.09	(Inyinbor et al., 2019)
Raw *Raphia hookeri*	81.97	(Inyinbor et al., 2019)
Modified pineapple bran	28.99	(Zhuang et al., 2020)
Modified Montmorillonite	30.72	(Chu et al., 2020)
Rubber leaf powder	9.07	(Rukayat et al., 2021)
Modified Irvingia gabonensis	73.53	This study

adsorbed at equilibrium were 12.91, 30.02, 44.98, 57.33 and 76.32 mg/g for initial concentration of 20, 40, 60, 80 and 100 mg/L respectively (Fig. 5). The high driving force at high concentration as well as the continuous surface bombardment at increased time may have resulted into increased metal uptake. Previous report by the works of Siddiqui (Siddiqui, 2018) which used *Luffa actangula* for the uptake of Cu^{2+} agrees with current findings.

3.2. Isothermal studies of Cu^{2+} adsorption onto EIG

Isotherm studies of the Cu2+-EIG system depict a compliment that suggests a multilayer adsorption as the R2 values for the Freundlich isotherm and D-R model were obtained to be 0.9322 and 0.9733 respectively (Ayawei et al., 2017). The favourability of the adsorption process has been justified by calculating the dimensionless RL value (Table S1), the RL value obtained (0.1091). The maximum monolayer adsorption capacity (qmax) was obtained to be 73.53 mg/g, this compare outstandingly with other studies using agricultural waste for Cu2+ adsorption (Table 1). The adsorption energy gotten from the D-R model read 5.51 kJ/mol, this indicates a physisorption of Cu2+ onto EIG.

3.3. Kinetics of Cu^{2+} uptake onto EIG

The kinetics studies of the Cu^{2+}-EIG system was on varying concentration. The constant α of the Elovich model relates to the chemisorption rate varied; α was found to be irregularly across the initial concentrations studied. This may suggest that chemisorption less occur in the Cu^{2+}-EIG adsorption system. Similarly, the pseudo second order kinetics model gave R^2 very close to unity as well as low values for X^2 and SSE (Table S2) hence the adsorption data fitted best into the pseudo second order kinetic model. The pseudo second order kinetics model represents adsorbate removal by physisorption (Robati, 2013). This corroborates the findings recorded in the isothermal studies of Cu^{2+}-EIG adsorption data. Close agreement also exists between values of quantity adsorbed at equilibrium as obtained by experimental for each concentration and their calculated counterparts for the pseudo second order kinetics model. The intercepts of the intraparticle diffusion model plot were greater than zero, this suggests that some degree of boundary layer diffusion in the Cu^{2+}-EIG system. The parameter C of the intraparticle diffusion model explains the boundary layer thickness; this parameter increased as the initial adsorbate concentration increased from 20 mg/L to 100 mg/L. This indicates that less degree of boundary layer control occurred at low initial adsorbate concentration.

3.4. Temperature effects on Cu^{2+} uptake onto EIG

The quantity of Cu^{2+} removal was found to slightly increase with temperature (Fig. 6). Temperature may have activate a few more site for adsorption. EIG however is highly potent at low temperature, about 98 % removal was recorded at temperature of 40 °C. Increased adsorbate uptake with temperature has been traced to surface site activation as well as increase in mobility of the Cu^{2+} due to increase in solution temperature. This also suggests that adsorption was more of physical than chemical.

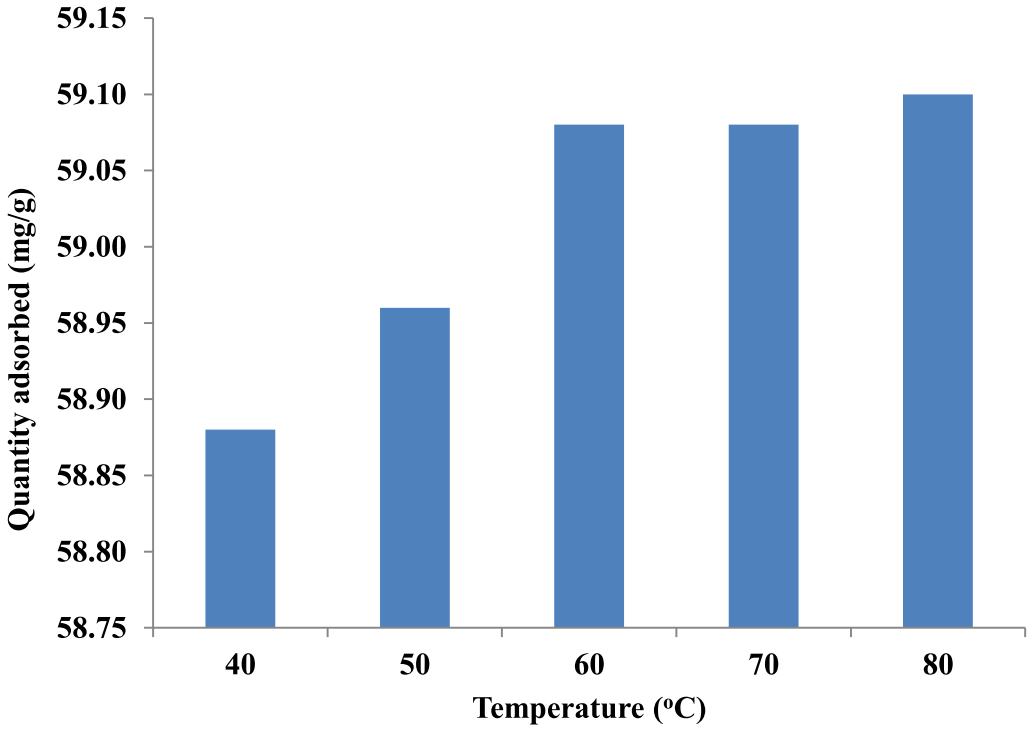

Fig. 6. Temperature effects on the efficiency of EIG for Cu2+uptake.Conditions: Dosage (1 g/L), Agitation speed (200 rpm), agitation time (120 minutes), a 60 mg/L Cu2+ solution, pH 5.

Table 2
Thermodynamics parameters for Cu2+-EIG adsorption system.

Adsorbent	ΔH^o (kJ/mol)	ΔS^o (J/mol/K)	ΔG^o (kJ/mol)				
			313	323	333	343	353
EIG	5.29	50.03	-10.31	-10.84	-11.52	-11.87	-12.28

Table 3
Correlation analysis output

	Concentration	Equilibrium time	Quantity adsorbed	
Concentration	Pearson Correlation	1	.894*	.998**
Equilibrium time	Pearson Correlation	.894*	1	.918*
Quantity adsorbed	Pearson Correlation	.998**	.918*	1

*Correlation is significant at the 0.05 level (2-tailed)
**Correlation is significant at the 0.01 level (2-tailed)

3.5. Thermodynamic Studies of Cu^{2+}-EIG adsorption system data

The practicality as well as the energy generation in the form of heat of the adsorption process is premised on parameters obtained from the Van't Hoffs plot (Fig. not shown). The uptake of Cu^{2+} onto EIG was endothermic in nature hence the positive value of ΔH^o. The feasibility and spontaneity of the adsorption process was established by the negative values of ΔG^o at all temperature studied (Table 2). The ΔG^o and ΔH^o whose values were less than 15.98 kJmol^{-1} and less than 40 kJmol^{-1} respectively expressly validated physical adsorption process in the Cu^{2+}-EIG system. The value of ΔS^o being positive suggests an increase in rate of disorderliness at the solid-liquid interphase.

3.6. Statistical validation of Process Operational Parameters

The statistical analysis in this section was conducted using R and SPSS Statistics 22. The result from Table 3 shows that a high positive and significant relationship exist between concentration, equilibrium time and quantity adsorbed onto EIG. The model parameter in Table 3 is estimated using the conventional ordinary least squares estimator (OLSE) on all the dataset. The preliminary diagnostic check in Table 4 revealed the tendency for the predictors (equilibrium time and concentration) to be correlated. The condition index for equilibrium time is higher than ten (10), it is evident that the predictors are correlated (Lukman et al., 2019). From Table 4, it is evident that quantity adsorbed increased as concentration and equilibrium time increases, respectively. F-test shows that the overall model fit well to the data since the p-value is less than 5% level of significance. The coefficient of determination (R2) revealed that the concentration and equilibrium time explains about 99% of the variation of quantity adsorbed hence a balance for economical process. In practical terms, EIG should be highly effective for Cu2+ uptake even in highly concentrated solutions. However, due to the presence of correlated predictors detected by high R2, highly positive correlation coefficient and the condition index, the ridge regression estimator is adopted (Hoerl and Kennard, 1970; Lukman et al. 2021). The ridge estimator has a tuning parameter, k. We divided the dataset into a training and a test set. Model fitting and tuning parameter selection by five-fold cross-validation were carried out on the training data (Arashi et al., 2021). We compared the ridge regression estimator (Ridge) and the ordinary least squares estimator (OLSE) via the test mean squared error (TMSE). The estimator with the smallest TMSE is preferred. The glmnet and the tidymodels libraries in the R software are employed. The result is provided in Table 5.

The result in Table 5 using the regularization techniques shows that the intercept of ordinary least squared estimate is negative while that of the ridge estimate is positive. Following Lukman and Ayinde (2017), one of the consquences of correlated predictors is wrong sign. Thus, the negatve sign by the OLS estimate might be attributed to this problem. The intercept of the ridge estimate revaled that there are other predictors that contributed to the quantity absorbed. Also, the ridge estimator is preferred in this study because the test mean squared error is smaller. From Table 5, it is evident that quantity adsorbed increased by about 68% and 28% as concentration and equilibrium time increases, respectively.

Table 5
Regression coefficients and TMSE

Coef.	OLSE	Ridge
Intercept	-0.0082	0.0072
Concentration	0.8842	0.6857
Equilibrium time	0.1419	0.2757
TMSE	0.0017	0.0003

Table 6
Regression Modelling of Temperature on Quantity adsorbed

Model		Unstandardized Coefficients		t	Sig.
		B	Std. Error		
1	(Constant)	45.489	6.012	7.566	.002
	Temperature	.205	.105	1.959	.122

Table 7
Regression modelling of time on Quad.

Concentration	Model	Unstandardized Coefficients	
		B	Std. Error
20	Intercept	9.858	1.888
	Time	.036	.034
40	Intercept	23.442	4.488
	Time	.079	.081
60	Intercept	29.916	5.740
	Time	.166	.104
80	Intercept	43.941	8.416
	Time	.160	.152
100	Intercept	57.496	11.011
	Time	.221	.199

Table 4
Regression coefficients and Diagnostic test

OLSE Coefficients[a] Model		Unstandardized Coefficients		t	Sig.	Collinearity Statistics	
		B	Std. Error			Eigenvalue	Condition Index
1	(Constant)	-9.838	2.575	-3.821	.062	2.898	1.000
	Concentration	.683	.030	22.747	.002	.096	5.487
	Equilibrium time	.147	.045	3.274	.082	.006	22.857
R^2	0.999	F-test	1653.507 (0.001)				

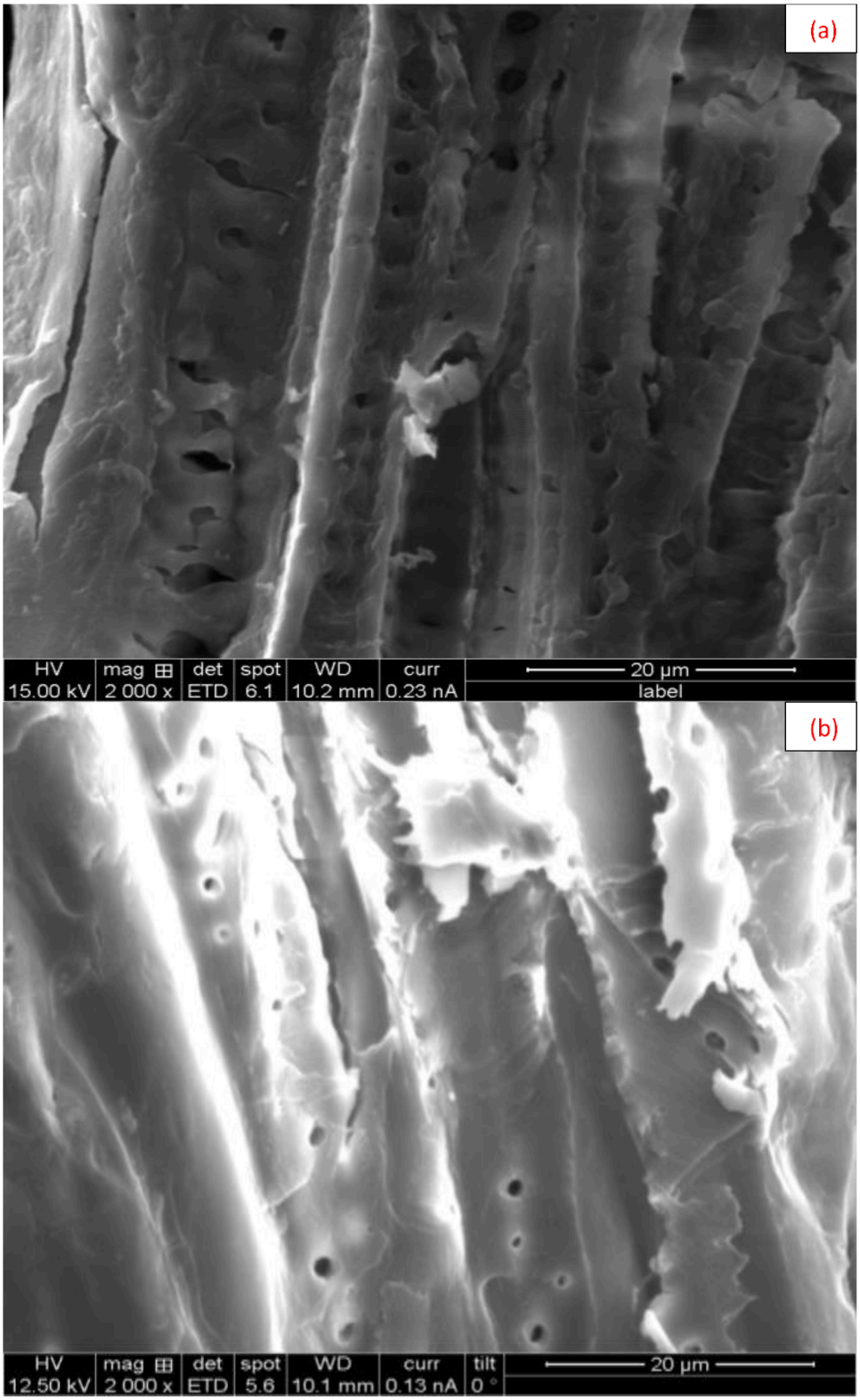

Fig.7. EIG surface morphology before Cu2+ adsorption (a) and after Cu2+ adsorption (b)

3.6.1. 3.6.1 Operational parameter and process economy: The temperature effect

The result in Table 6 shows that temperature has a positive impact on quantity absorbed. As temperature increase by 1 unit, quantity adsorbed increases by about 20.5 %. Although, high energy requirement has cost implications. However, if a unit increase in energy raises adsorption capacity of EIG by 20.5 %, then the energy cost would become negligible thus presenting an economical process. We also examined the effect of time on quantity absorbed at different concentrations. The result is presented in Table 7 The result shows that time made the highest impact on quantity adsorbed when the level of concentration is 100 mg/L while the lowest impact was recorded when the concentration level is 20 mg/

L.

3.7. Desorption studies of Cu^{2+}-EIG system

In order to improve the process economy, three eluent were used to establish an effective desorption system. Percentage desorption was found to be generally low. Only 0.38 % Cu^{2+} desorption was obtained using neutral H_2O, 1.2 % Cu^{2+} desorption was obtained for HCl while desorption with acetic acid gave 1.65 % Cu^{2+} desorption. Hence, EIG may be a once and for all usage. The wide availability of dika fruit may be effectively compensate for this in process economy.

3.8. Comparing the morphological appearance and surface chemistry of EIG before and after Cu^{2+} uptake

The heavy gullies on the surface of EIG before Cu^{2+} uptake had been covered after Cu^{2+} adsorption (Fig.7 a and b). Swollen fibers also characterized the post adsorption EIG. Fibers and pores plays significant role in pollutants uptake. The BET surface area of EIG was found to be significantly low (Table 2), hence, the uptake/removal of Cu^{2+} may have been primarily by pore penetration and fiber loading. The bands of the –OH, C-OH, C=O and C-H stretching vibrations observed on EIG had shifted positions after Cu^{2+} uptake (Fig. S1), this suggests that the functional groups may have also played some sorptive roles.

4. Conclusion

Surface functionalization of Irvingia gabonensis biomass impacted relevant functional groups on the biomass surface leading to low BET surface area. Morphology of EIG revealed fibrous nature of agrowaste and these fibers participated in Cu2+ uptake. Optimum adsorption was obtained at pH of 5. Isothermal analysis of adsorption data suggests that adsoprion was onto multiple surface and physisorption predominate the Cu^{2+}-EIG system. The q_{max} was 73.53 mg/g and this compares well with previously reported works. Although, adsorption operational parameter as well as statistics showed that high temperature favoured the uptake of Cu^{2+} onto EIG; the multiple percentage adsorption increase at a unit temperature increase justifies that Cu^{2+}-EIG adsorption process at high temperature would be economical.

Declaration of Competing Interest

The authors declare that they have no known competing financial interests or personal relationships that cdocould have appeared to influence the work reported in this paper.

Supplementary materials

Supplementary material associated with this article can be found, in the online version, at https://doi.org/10.1016/j.sajce.2022.03.001.

References

Aharoni, Ungarish, 1976. Kinetics of activated chemisorption: Part 1.-The non-elovichian part of the isotherm. Journal of the Chemical Society, Faraday Transactions 1 72, 400–408. https://doi.org/10.1039/F19767200400. Physical Chemistry in Condensed Phases.

Arashi, Asar, Yüzbaşı, 2021. SLASSO: a scaled LASSO for multicollinear situations. Journal of Statistical Computation and Simulation. https://doi.org/10.1080/00949655.2021.1924174.

Avrami, 1940. Kinetics of phase change. II Transformation-time relations for random distribution of nuclei. The Journal of Chemical Physics 8 (2), 212–224. https://doi.org/10.1063/1.1750631.

Ayawei, Ebelegi, Wankasi, 2017. Modelling and Interpretation of Adsorption Isotherms. Journal of Chemistry 2017. https://doi.org/10.1155/2017/3039817.

Cid, Flores, Pizarro, Castillo, Barros, Moreno-Piraján, Ortiz, 2018. Mechanisms of Cu2+ biosorption on Lessonia nigrescens dead biomass: Functional groups interactions and morphological characterization. Journal of Environmental Chemical Engineering 6 (2), 2696–2704. https://doi.org/10.1016/j.jece.2018.03.034.

Dubinin, Radushkevich, 1947. Equation of the characteristic curve of activated charcoal proceedings of the academy of sciences. Physical Chemistry Section, USSR 55, 331–333.

El-Shafey, Al-Busafi, Al-Lawati, Al-Shibli, 2017. Removal of Cu2+ and SO42− from aqueous solutions on surface functionalized dehydrated carbon from date palm leaflets. Journal of Water Process Engineering 15, 62–71. https://doi.org/10.1016/j.jwpe.2016.08.007.

Fawzy, 2020. Biosorption of copper ions from aqueous solution by Codium vermilara: Optimization, kinetic, isotherm and thermodynamic studies. Advanced Powder Technology, xxxx. https://doi.org/10.1016/j.apt.2020.07.014.

Fazlzadeh, Khosravi, Zarei, 2017. Green synthesis of zinc oxide nanoparticles using Peganum harmala seed extract, and loaded on Peganum harmala seed powdered activated carbon as new adsorbent for removal of Cr(VI) from aqueous solution. Ecological Engineering 103, 180–190. https://doi.org/10.1016/j.ecoleng.2017.02.052.

Flanagan, Branchu, Boudahmane, Caupos, Demare, Deshayes, Dubois, Kajeiou, Meffray, Partibane, Saad, Lima, Gromaire, 2019. Stochastic method for evaluating removal, fate and associated uncertainties of micropollutants in a stormwater biofilter at an annual scale. Water (Switzerland) 11 (3). https://doi.org/10.3390/w11030487.

Freundlich, 1906. Over theadsorption in solution. Z. Phys. Chem. 57, 385–470.

Gajda, Stinchcombe, Greenman, Melhuish, Ieropoulos, 2017. Microbial fuel cell – A novel self-powered wastewater electrolyser for electrocoagulation of heavy metals. International Journal of Hydrogen Energy 42 (3), 1813–1819. https://doi.org/10.1016/j.ijhydene.2016.06.161.

Hayati, Maleki, Najafi, Daraei, Gharibi, McKay, 2017. Adsorption of Pb2 +, Ni2 +, Cu2 +, Co2 + metal ions from aqueous solution by PPI/SiO2 as new high performance adsorbent: Preparation, characterization, isotherm, kinetic, thermodynamic studies. Journal of Molecular Liquids 237, 428–436. https://doi.org/10.1016/j.molliq.2017.04.117.

Ho, McKay, 1999. Pseudo-second order model for sorption processes. Process Biochemistry 34 (5), 451–465. https://doi.org/10.1016/S0032-9592(98)00112-5.

Hoerl, Kennard, 1970. Ridge regression: Biased Estimation for Non-Orthogonal Problems. Technometrics 12, 55–67 https://www.tandfonline.com/doi/abs/10.1080/00401706.1970.10488634.

Inyinbor, A A, Adekola, Olatunji, 2015. EDTA Modified Irvingia g abonensis : An Efficient Bioresource Material for the Removal of Rhodamine B. Pak. J. Anal. Environ. Chem. 16 (2), 38–47.

Inyinbor, Adejumoke Abosede, Adekola, Olatunji, 2019. Copper scavenging efficiency of adsorbents prepared from Raphia hookeri fruit waste. Sustainable Chemistry and Pharmacy 12, 100141. https://doi.org/10.1016/j.scp.2019.100141. December 2018.

Kajeiou, Alem, Mezghich, Ahfir, Mignot, Devouge-Boyer, Pantet, 2020. Competitive and non-competitive zinc, copper and lead biosorption from aqueous solutions onto flax fibers. Chemosphere 260. https://doi.org/10.1016/j.chemosphere.2020.127505.

Lagergren, 1898. On the theory of so-called adsorption of dissolved substances. Kungliga Svenska Vetenskapsakademiens Handlingar 24 (4), 1–39.

Langmuir, 1917. The constitution and fundamental properties of solids and liquids. Journal of the Franklin Institute 183 (1), 102–105. https://doi.org/10.1016/S0016-0032(17)90938-X.

Lin, Wang, Zhang, Hu, Cheng, Fu, Xiong, 2019. Enhanced and selective adsorption of Hg2+ to a trace level using trithiocyanuric acid-functionalized corn bract. Environmental Pollution 244, 938–946. https://doi.org/10.1016/j.envpol.2018.08.054.

Lucaci, Bulgariu, Ahmad, Lisa, Mocanu,, Bulgariu, 2019. Potential use of biochar from variouswaste biomass as biosorbent in Co(II) removal processes. Water (Switzerland) 11 (8). https://doi.org/10.3390/w11081565.

Lukman, Ayinde, Binuomote, Clement, 2019. Modified Ridge-Type Estimator to Combat Multicollinearity: Application to Chemical Data. Journal of Chemometrics 33 (5), e3125. https://doi.org/10.1002/cem.3125.

Lukman, Adewuyi, Månsson, Kibria, 2021. A new estimator for the multicollinear poisson regression model: simulation and application. Scientific Reports 11, 3732. https://doi.org/10.1038/s41598-021-82582-w.

Robati, 2013. Pseudo-second-order kinetic equations for modeling adsorption systems for removal of lead ions using multi-walled carbon nanotube. Journal of Nanostructure in Chemistry 3 (1). https://doi.org/10.1186/2193-8865-3-55.

Siddiqui, 2018. The removal of Cu2+, Ni2+ and Methylene Blue (MB) from aqueous solution using Luffa Actangula Carbon: Kinetics, thermodynamic and isotherm and response methodology. Groundwater for Sustainable Development 6, 141–149. https://doi.org/10.1016/j.gsd.2017.12.008. August 2017.

Soliman, Mohamed, Ahmed, Sayed, Elghandour, Ahmed, 2019. Cd 2+ and Cu 2+ removal by the waste of the marine brown macroalga Hydroclathrus clathratus. Environmental Technology and Innovation 15, 100365. https://doi.org/10.1016/j.eti.2019.100365.

Tan, Sun, Hu, Fang, Bi, Chen, Cheng, 2015. Adsorption of Cu2+, Cd2+ and Ni2+ from aqueous single metal solutions on graphene oxide membranes. Journal of Hazardous Materials 297, 251–260. https://doi.org/10.1016/j.jhazmat.2015.04.068.

Tavakoli, Goodarzi, Saeb, Mahmoodi, Borja, 2017. Competitive removal of heavy metal ions from squid oil under isothermal condition by CR11 chelate ion exchanger. Journal of Hazardous Materials 334, 256–266. https://doi.org/10.1016/j.jhazmat.2017.04.023.

Vinet, Zhedanov, 2011. A “missing” family of classical orthogonal polynomials. Journal of Physics A: Mathematical and Theoretical 44 (8), 327–356. https://doi.org/10.1088/1751-8113/44/8/085201.
Weber, 1963. Kinetics of Adsorption on Carbon from Solution. Journal of the Sanitary Engineering Division 89 (2), 31–60.
Xiong, Wang, Sun, Li, 2019. Selective adsorption of Pb(II) from aqueous solution using nanosilica functionalized with diethanolamine: Equilibrium, kinetic and thermodynamic. Microchemical Journal 146, 270–278. https://doi.org/10.1016/j.microc.2019.01.005. December 2018.